

Classification Of Hand Images by Person, Age and Gender with The Median Robust Extended Local Binary Model

Emrah Aydemir and R.T. Esfandiyar Alalawi


Abstract— Biometric technologies try to automatically recognize individuals by considering the physiological and behavioral characteristics of individuals. Although the methods used here are very diverse, the personal qualities used also vary. Facial features, finger and vein prints, iris, retina, ear, hand, and finger recognition are only some of the physiological features. It may be preferred to use one or more of these personal features to reduce the margin of error that may arise depending on the security level in the applications used. Biometric recognition systems have varying requirements in security systems applications. Fingerprint and iris recognition work well in applications that require high security levels, while applications that require low security levels are not suitable due to privacy concerns. On the other hand, identification from hand images is more accepted based on the idea that it does not have a very high distinctiveness. But it is sufficient for medium security applications. Apart from these, palm images have many advantages such as reliability, stability, user-friendliness, non-intrusiveness, and flexible use. In this study, it is aimed to identify people, determine their ages, and determine their gender by using both upper surface and inner surface images of right-left hand data of hand shape. For this purpose, images of both the inner surface of the hand (10) and the outer surface of the hand (10) of 100 different people were collected. This was done separately for the right and left hands, and a total of 3955 images were obtained. The features of these images were extracted using the Median Robust Extended Local Binary Model (MRELBP). Images are classified for person, age and gender. The results were 91.4%, 85.9% and 92.6%, respectively.

Index Terms— Hand image, Median Robust Extended Local Binary Model, MRELBP, Classification.


I. INTRODUCTION

BIOMETRIC IDENTIFICATION has become inevitable due to rapid developments in the world and increasing security requirements.

EMRAH AYDEMİR, is with Department of Electrical Engineering University of Sakarya University, Sakarya, Turkey, (e-mail: emrahaydemir@sakarya.edu.tr).

 <https://orcid.org/0000-0002-6598-7251>

RAGHAD TOHMAS ESFANDIYAR ALALAWI, is with Department of Computer Engineering, Ahi Evran Uni., Kirsehir, Turkey, (e-mail: alalawiraghad@yahoo.com).

 <https://orcid.org/0000-0002-6598-7251>

Manuscript received September 6, 2022; accepted November 22, 2022.

DOI: [10.17694/bajece.1171905](https://doi.org/10.17694/bajece.1171905)

Now, the sustainability of security is low with the records kept in the books or traditional applications such as photographs, identity cards and signatures. It has become a necessity to carry out these processes with computer-based systems that will reduce human error. In addition to keeping records in various databases, digitally obtained biometric data should be used for person verification. These systems will be able to see the small details and differences that the human eye misses much better. For this, they match the data stored in the databases. Such systems have become frequently encountered in daily life. In many countries, palm, eye, fingerprint, etc. automatically at airports and border gates. biometric recognition systems are used. Similarly, in many countries, studies are carried out to record biometric data in passports [1].

There are many advantages to using biometric data to identify people. The most important of these are the uniqueness of biometric data and having a fixed shape. As the demand for biometric recognition systems increases, the demand for the evaluation of their performance also increases accordingly. However, not all biometric recognition systems have the same advantages. For the most widely used fingerprint recognition systems, the finger is expected to be clean and free of various stains. Such situations negatively affect performance [2]. Interest in ear recognition studies and their conversion to commercial technologies is low for several reasons [3, 4]. Like many other biometric features, palm shape changes little with age. In addition, the veins on and outside the palm are also used as a unique element in person recognition [5]. Because the vein patterns are based on the body's internal biological information, they are not affected by the destructions of the outer surface and cannot be easily copied. This increases its reliability as a biometric recognition feature. The appearance of these checkers in different individuals is a distinctive feature [6].

The palm consists of the inner surface of the hand between the wrist and the fingers. This inner surface consists of three parts: finger root region, inner region and outer region. There are three main lines on the palm that are formed because of flexing the hand. These are the life line, the heart line, and the head line [7]. These lines and accompanying wrinkles and secondary lines become more distinctive over time. It characterizes people because of their stable nature. An example palm image is given in the figure below.

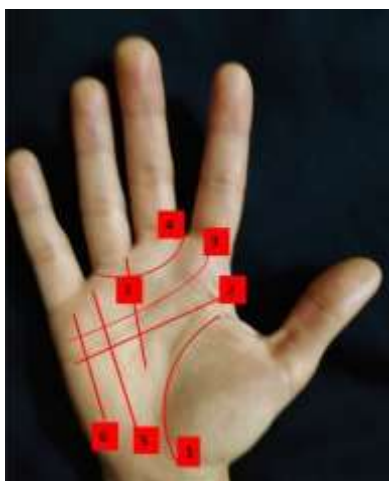


Fig. 1. An example palm shape and lines

The number of lines on the palms, their relationships and distances are the main features used in authentication. Figure 1 above shows both the three main lines and the crumpled lines. The names of the lines given with numbers on the figure are as follows.

1. Lifeline
2. Headline
3. Heart Line
4. Belt of Venus
5. Sun Line
6. Mercury Line
7. Destiny Line

In addition to being authentic, they are practical for authentication, as the lines on the palm are more pronounced rough lines. It offers the opportunity to work quickly and flexibly even with lower resolution images [8]. Systems that extract features from palm images by focusing only on line structures have certain disadvantages. Some of these are the indistinct palm prints, palm prints with similar line features, and ignoring the thickness and width of the lines [9]. Wrinkles and fine ridges can be analyzed with a medium resolution, although low resolution is not a problem because the main lines in the palm images are thick.

Chiromancy is the study of the size, shape and appearance of the hand, including analysis of the color, texture and elasticity of the skin. Chiromancy studies begin with recognizing the basic hand shapes. Evaluation of hand shape gives an idea about the basic character of the individual, and throughout history, palmists have developed various classification systems for hand types [10]. Saint -Germain [11] classified basic personalities according to hand types. Finger proportions, hand lines and other factors are considered here.

Knowing the shapes of people's hands and palms means that these processes can be easily determined by computer-based systems. Fingers and fingerprints are also involved in the recognition systems of the inner and outer surfaces of the hand. Fingerprints are caused by the different growth and pressure experiences of the embryo inside the womb. Therefore, it differs even for identical twins [12, 13]. Folds, angles and distances in fingerprints are used for identification [14]. But for this, the image must be clear enough to distinguish these subtleties.

A. Aim

Biometric technologies try to automatically recognize individuals by considering the physiological and behavioral characteristics of individuals. Although the methods used here are very diverse, the personal qualities used also vary. Facial features, finger and vein prints, iris, retina, ear, hand and finger recognition are only some of the physiological features. It may be preferred to use one or more of these personal characteristics in order to reduce the margin of error that may arise according to the security level in the applications used [15]. Biometric recognition systems have varying requirements in security systems applications. Fingerprint and iris recognition work well in applications that require high security levels, while in applications that require low security levels, they are not suitable due to privacy concerns. On the other hand, identification from hand images is more accepted based on the idea that it does not have a very high distinctiveness. But it is sufficient for moderate security applications [16]. Apart from these, palm images have many advantages such as reliability, stability, user-friendliness, non-intrusiveness and flexible use. In this study, it is aimed to identify people, determine their ages and determine their gender by using both the upper surface and inner surface images of the right-left hand data of the hand shape.

B. Literature review

Images from palm prints are available from Fei et al. [17] using the multi-layered direction subtraction method. With this method, firstly, the apparent direction on the surface layer of the palm print is obtained, and then the hidden features in the energy map layer of the visible direction are used. The histogram of both features is extracted and PolyU 98.83% recognition success is achieved with the dataset. PolyU with the same dataset multispectral palm print images Cui [18] with the fusion strategy. Here, images are captured in red, green, blue and near infrared, respectively. Thus, it contains more information compared to other images. It used the expanded general color image discriminant (GCID) model to generate three new color components to further improve the recognition performance, achieving 99.57% success. Zhang and Gu [19] proposes to combine competitive coding method and two-step test sample sparse representation (TPTSR) method for palmprint recognition. The TPTSR method, which is one of the representative methods, takes the entire palm image as input and determines the contribution of the training samples of each class in representing the test sample. TPTSR also uses the corresponding contribution values to calculate the similarities between the test sample and each class. The competitive coding method is a feature-based method and is highly complementary to TPTSR. The author uses a weighted fusion scheme to combine the matching scores generated from the TPTSR and competitive coding method. Experimental results show that the proposed method can achieve a very high classification accuracy and outperform both TPTSR and competitive coding method. The method, validated with 6000 samples from 500 people (12 palms), and the match rate of TPTSR is presented, reveals a 94% success rate. Zhang and Gui [20] propose a palm recognition method based on representation in feature space in another study. The proposed method aims to represent the test

sample as a linear combination of all training samples in the feature space and then uses the resulting linear combination to perform palmprint recognition. The author applies the original space-to-feature space mapping using kernel functions such as the radial basis function (RBF). In this method, the selection of the kernel function's parameter is important. It proposes an automatic algorithm for selecting the parameter. The basic idea of the algorithm is to optimize the feature space such that while instances of the same class are clustered well, instances from different classes are pushed away. The proposed criterion measures the goodness of a feature space, and by minimizing this criterion, the optimal kernel parameter is obtained. Experimental results on the database achieved 98% success in the public dataset of the proposed methods.

Li, Cao and Lu [21] that the two-stage test sample representation method (TPTSR) performs very well. TPTSR is not only a competent representational classification method, but also computationally more efficient than the original sparse representation methods. However, although TPTSR seems suitable for palm recognition, it has not been widely tested and it is unknown how to set the parameter (number of nearest neighbors) which is absolutely crucial for real-world applications. The study aimed to analyze the performance of the method in palm identification. In this context, numerous experiments on palm recognition have been conducted to address the mentioned problems. The method was validated on the "PolyU" database and achieved low error rates. Zhao and Zhang [22] propose a general framework that represents high-level discriminating features for multiple scenarios in palmprint recognition with learned discriminating deep convolutional networks called deep discriminant representation (DDR). They use discriminant deep convolutional networks for learning, with limited palmprint training data used to extract deep discriminants. Next, the collaborative representation-based classifier for palmprint recognition is applied, which is flexible and practical in multiple scenarios. Experimental results show that DDR produces the best recognition performance in general palm recognition compared to other state-of-the-art methods. Over 98% results were obtained in the PolyU Multi-spectral database with DDR, M_R, M_B, M_G and M_NIR respectively for contact-based palm recognition under different lighting sources, and in DDR, IITD and CASIA databases for contactless palmprint recognition.

Matkowski, Chai, and Kong [23] to examine palmprint identification on images collected in an uncontrolled and uncooperative environment. It contains 2035 palms collected from the internet and obtained from 7881 images. The proposed algorithm consists of an alignment network and a feature extraction network and can be trained end-to-end. The algorithm was compared with state-of-the-art online palm recognition methods and evaluated on three common contactless palmprint databases, IITD, CASIA and PolyU, and two new databases, NTU-PI-v1 and NTU contactless palmprint database. The proposed algorithm achieved successful results in NTU-PI-v1, NTU-CP-v1, IITD, PolyU and CASIA databases at a rate of 41.92%, 95.34%, 99.61%, 99.77% and 97.65%, respectively. This system is sufficiently resistant to

noise and deformation [24]. In the identification system, ONPP is used for manifold learning and the point-to-manifold distance function is used to test the finger core. Based on the infrared image database TED -FV, the proposed method achieves 97.8% recognition rate with the identification pattern, which is better than other traditional methods. Experimental results have shown that the proposed system is an effective and robust method for its performance.

Hong et al. [25] multispectral palmprint instead of natural light palm print and developing a multi-band palm print recognition method based on a hierarchical idea, to achieve higher recognition rate with more distinctive information. First, Block-Based Routing Code (BDOC) as a rough feature, and Block-Based Directed Gradient as a good feature. They extract the histogram (BHOG). Secondly, a hierarchical recognition approach is proposed based on these two types of features. They combine different features from different bands in the proposed scheme to improve recognition accuracy. Finally, the experimental results show that the recognition accuracy of the proposed method is not only superior to previous high-performance methods based on the PolyU palm database with natural light but can further improve the state-of-the-art performance achieved by some approaches. Trying to refine coding-based approaches using multi-spectral palm print images, Bounanche et al. [26] presents a new multi-spectral palmprint recognition approach based on directed multi-scale log-Gabor filters. The proposed method aims to increase recognition performances by suggesting new solutions in three stages of the recognition process. Inspired by bitwise competitive coding, feature extraction uses multi-resolution log-Gabor filtering; where the final feature map consists of the winning codes of the bank response of the lowest filters. MS-PolyU EER results of less than 0.01 were obtained in the database. Ma et al. [27] introducing the idea of discrimination analysis into palm coding, they attempted to extract DOSFL, orientation and scale features with more appropriate discrimination. DOSFL then uses four code bits to represent both the orientation and scale characteristics of the palmprint and uses the Hamming distance for code matching. In order to make better use of the direction and scale information contained in the palm print samples, a discriminative learning (MOSDL) approach with versatile and multi-scale features for palm print recognition, which can effectively combine different orientation and scale feature data in the discriminative learning process, is proposed in this context. Experimental results on two publicly available palm databases, including the HK PolyU database and the UST image database, show that the proposed method can achieve better recognition results than the compared methods, with accuracy values of 98.05% and 97.63%, respectively.

Tamrakar et al. [28] presented an effective palm print recognition technique for palm prints collected with both visible and multispectral imaging systems. ROI extraction is a challenging task for palm print captured in unconstrained environment. ROI achieved by finger spacing and palm width makes system rotation and translation invariant. The

approximate ROI obtained by first-order decomposition of the ROI reduces the Haar wavelet computational overhead and noise. Phase quantization with Gaussian derivative filter of AROI gives the Gaussian derivative phase pattern image, and its block-based histograms are combined to form a single vector called the BGDPPH descriptor. Size reduction is achieved by increasing the distinction between genuine and dishonest scores using Chi -RBF kernel discriminant analysis (KDA). Weighted score level fusion of spectral palm prints in the Fisher criterion improves the recognition rate. The robustness of the proposed BGDPPH identifier against blur and noise has been validated on four grayscale and two multi-band palmprint databases collected via touch-based devices. It is stated in the study that when the proposed method is applied on these four different data sets, "PolyU 2D", "IIITDMJ", "CASIA", and "IITD" accuracy rates of 99.98%, 100%, 99.22%, and 99.19%, respectively. Hong et al. [29] presented a palm print recognition system using the fast Vese-Osher decomposition model to process blurry palm print images. First, a Gaussian blur distortion model (GDDM) is proposed to characterize image blur, and from this model it is observed that there are some stable features in palm images with different blur scale. Second, the structure layer and texture layer of blurred palm print images are obtained using the fast Vese-Osher decomposition model, and the structure layer proves to be more stable and robust than the texture layer for palm recognition. As a result, a new algorithm based on the weighted histogram of the directed gradient for the locally selected model (WHOG-LSP) is proposed and used to extract some robust features from the structure layer of the blurred palm print images. These extracted features were used to fix poor performance issues associated with translation and rotation in palm print recognition. Finally, the normalized correlation coefficient (NCC) was used to measure the similarity of palm features for the proposed recognition system. Extensive experiments on the PolyU palm database and the fuzzy PolyU palm database confirm the effectiveness and real-time feasibility of the proposed recognition system. Additionally, IIT Delhi Touchless An experiment was conducted to verify the robustness of the proposed method in the Palmprint database and EER values of 0.0727 % and 0.9210 were obtained, respectively.

II. MATERIAL AND METHOD

A. Data Gathering

Before starting the study, the people who will collect image data were informed about the purpose of the study and how the data will be used. It was stated that there was voluntary participation, and it was clearly explained that no data that could identify him, such as his name or surname, would be collected. Voluntary participants were asked to press the inner and outer surfaces of each hand on a piece of black cloth. In the study, image data of both the palm and the upper surface of the hand of 100 different people were collected. A total of 40 images were obtained from a person, 10 for the left and right palms, and 10 for the upper surface of the hand. In this way, 3955 images were obtained. In the images that were examined

later, it was seen that 5 files had the same name, and they were deleted because it was not known exactly to which user they belonged. For this reason, the number of files that should have been 4000 in total became 3955. Images were obtained from different angles with a high-resolution device. Only age and gender information were obtained from the people whose images were taken. Apart from this, no data to identify individuals was recorded. In order to determine who the people are, a sequential ID number in the range of 1-100 is given. A naming convention has been developed for the name of each image file so that there are many images and no name confusion. According to this rule, people's ID numbers, ages, genders and sequence number of the captured image are used. The underscore (_) character is used to legibly parse each data. Here, the following rules have been applied respectively.

- **Person ID:** It is a unique code value for each person photographed. This value ranges from 1 to 100.
- **Age:** The age is written directly as a number to express how old the person is.
- **Gender ID:** It is expressed with the value of 1 if the person photographed is male, and 0 if it is a female.
- **Photo ID:** Since more than one image was taken of each person, each image was numbered sequentially from 1 to 40.

The inner and outer surface images of the left hand of the person with the ID number 49 are shown in the figure below.



Fig. 2. Inner and outer space surface view of a sample person's hand

Naming the files according to the naming convention both prevents confusion and makes it easier to determine which class they belong to during the analysis. In the figure below, some of the image files are shown in the folder.



Fig. 3. folder view of the captured image files

For the data collected in the study to be used by other researchers, all image files were uploaded to the KAGGLE dataset repository. This dataset can be downloaded from www.kaggle.com/dataset/c1b48bedfa86c1b51e6acafe8c75e08

c01dbdf7d2444a07428540ece310b8163 and used by citing this study.

B. Analysis of Data

In order to make simple statistical analyzes from the data collected in the study, first of all, the file names were transferred into an excel file. Thus, each data name in the filenames has been split into columns. Python program was used for these operations. In the analysis of the data, a computer with Windows operating system, 40GB RAM and Intel(R) Core (TM) i7-8565U CPU, 1.80GHz 1.99GHz processor and 1TB SSD was used. First of all, simple statistical findings belonging to person, gender and age categories were obtained over the file names. Thus, the distribution of the data was examined. Then, the Median Robust Extended Local Binary Model (Median) is used for feature extraction from the image files. robust extended local binary Pattern -MRELBP) method was used. Local Binary Pattern (LBP), Local Phase Quantization (LPQ), Local Ternary Pattern (LTP) and MRELBP feature extraction methods are used with Subspace KNN classification algorithm. Success rates in person classification were found to be 75.1, 76.2, 61.9, and 79.3, respectively. This method was used because the highest accuracy rate was obtained in the MRELBP method. This method [30] as a tool in the Matlab program. Thus, 1x800 vectors were produced for each image file. This process has been done for all files. First, to identify people from hand images, person ID values were written as classification tags in these files. Then, another attribute file was created, and gender was written as the class label, and another file was created, and age was written as the class label. Thus, three different attribute files were obtained. Images are not separated as the inner surface or outer surface of the hand, nor are they separated as right and left hands. The data were separated into training and testing using the 10-fold cross-validation method. Then, these feature files were tested with 32 different classification algorithms in the Matlab program. The highest classification success was tried to be achieved. For classification processes, only one learning and testing process was performed. Repeated attempts were not made to achieve a higher success rate. In the title of Findings, each classification algorithm and the success rate obtained are given.

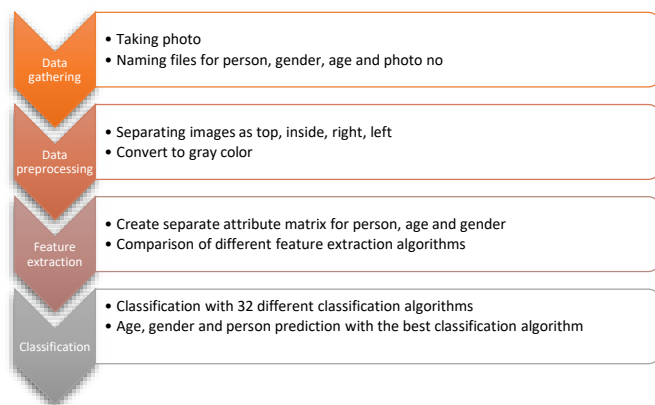


Fig. 4. Operation method and steps

The classification algorithms used are listed below. Default parameters are used by Matlab for these algorithms.

- Fine Tree

- Medium Tree
- Coarse Tree
- Linear Discriminant
- Quadratic Discriminant
- Logistics Regression
- Gaussian Naive Bayesian
- Kernel Naive Bayesian
- Linear Svm
- Quadratic Svm
- Cubic Svm
- Fine Gaussian Svm
- Medium Gaussian Svm
- Coarse Gaussian Svm
- Fine Knn
- Medium Knn
- Coarse Knn
- Cosine Knn
- Cubic Knn
- Weighted Knn
- Boosted Trees
- Bagged Trees
- Subspace Discriminant
- Subspace Knn
- Rusboosted Trees
- Narrows Neural Network
- Medium Neural Network
- Wide Neural Network
- Bilayered Neural Network
- Tripping Neural Network
- Svm Kernel
- Logistics Regression Kernel

C. Feature Extraction with Median Robust Extended Local Binary Model Extraction of Median robust extended local binary Pattern -MRELBP)

Local binary patterns (LBP) are an image processing algorithm that extracts texture features from images and uses them to classify and segment images. This algorithm was first proposed by computer scientists Oyala and Pettenkainen in 1994. Since then, this algorithm has evolved to include: It was used to extract the Tissue feature from 3D images and video clips and to recognize faces in medical images and identify diseases. Local binary patterns are calculated for a texture image in its simplest form as follows:

- First of all, the neighborhood system next to each pixel is used. That is, 8 values around the midpoint of a 3x3 matrix are taken into account.
- Each of the adjacent points (eight points) is compared to the center point. The value “0” is stored if the center point is larger, otherwise “1” values are retained.
- Finally, these 1 and 0 values obtained for each pixel in the image are converted to a decimal number. Thus, the LBP code consisting of decimal numbers is generated for each pixel.
- A histogram of all decimal values in the image is created, which is then used as a description of the entire image texture.

An example of a pixel for the above-mentioned calculation is given with steps in the figure below.

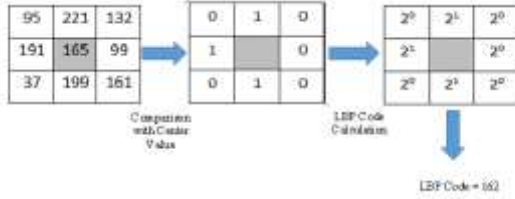


Fig. 5. LBP Sample Calculation

The following mathematical formulas are used to calculate the LBP code.

$$LBP_{8,1}(x_c) = f(x) = a_0 + \sum_{p=0}^{p-1} u(u(x_p - x_c))^{2^p} \quad (1)$$

$$u(y) = \begin{cases} 1 & y \geq 0 \\ 0 & y < 0 \end{cases} \quad (2)$$

In these equations, it is used to express the difference between the neighboring pixel and the center pixel y , the LBP tag represents the generated center pixel x_c , it x_p is expressed by the neighbors of the center pixel, $u(y)$ the result is the result, and here the result is the result of the LBP operator [31].

The upper version of LBP, ELBP, is designed to calculate distinctive spatial relationships in a local region. LBP, on the other hand, only calculates the relationship between neighbors and a central point. For these reasons, the ELBP method contains more spatial information than LBP. In addition, ELBP consists of three parts. With ELBP_CI, the central pixel is taken and the relationship with the neighbors is calculated accordingly. The following equation is used for this calculation.

$$ELBP - CI_{r,p}(x_c) = \sum_{n=1}^{\infty} s(x_c - \beta) \quad (3)$$

In ELBP_NI, on the other hand, instead of calculating the central pixel, the average of the neighbors is calculated, and this creates a serious functional difference from the LBP. The ELBP_NI formula is given in Equation 4.

$$ELBP - NI_{r,p}(x_c) = a_0 + \sum_{n=0}^{p-1} s(x_{r,n} - \beta_{r,p})^{2^n} \quad (4)$$

Alongside the ELBP_CI and ELBP - NI values, the ELBP_RD value is also calculated. The ELBP_RD equation 2.5 derived from the pixel differences in the radial directions is calculated.

$$ELBP - RD_{r,r-1,p}(x_c) = \sum_{n=0}^{p-1} s(x_{r,p,n} - x_{r-1,p,n})^{2^n} \quad (5)$$

One of the ELBP's drawbacks is that it is very inefficient against image noise. That's why MRELBP was developed. The solution is to first replace the individual pixel intensities at a point with representation over a region. Also, a single pixel that is not very bright or has distorted noise can significantly affect the Gaussian smoothed value or average value of all neighboring pixels, resulting in unreliability of the binary code. For these reasons, MRELBP was developed. The created MRELBP consists of three parts MRELBP CI, MRELBP NI

and MRELBP RD.

$$MRELBP_{CI}(x_c) = s(\phi(X_{c,w}) - \mu_w) \quad (6)$$

$X_{c,w}$ Represents the central, $\phi(X_{c,w})$ average value for the area that specifies the x_c local patch. $w * w$

$$MRELBP_{NI,r,p}(x_c) = \sum_{n=0}^{p-1} s((\phi(X_{r,p,w_r,n}) - \mu_{r,p,w_r}))^{2^n} \quad (7)$$

$$\mu_{r,p,w_r} = \frac{1}{p} \sum_{n=0}^{p-1} \phi(X_{r,p,w_r,n}) \quad (8)$$

$X_{r,p,w_r,n}$ Specifies the $w * w$ local patch for area r, p, w_r, n centered pixels for neighbors.

$$MRELBP_{RD_{r,r-1,p,w_r,w_r-1}} = \sum_{n=0}^{p-1} s((\phi(X_{r,p,w_r,n}) - \phi(X_{r-1,p,w_r-1,n})))^{2^n} \quad (9)$$

MRELBP is very efficient and achieves very good results when compared to RELBP. The MRELBP has been extensively tested with different types of noise, such as Gaussian white noise, Gaussian blur, salt, pepper and pixel random distortion, and delivers very efficient results. Also, MRELBP has multiple very important features, and foremost among these is computational simplicity, as well as nice features like gray scale and rotation invariance. Finally, MRELBP shows efficient results very easily without pre-training and adjusting parameters, which means convenience for the user [32].

D. Success Criteria

Different criteria can be used to evaluate the success of machine learning algorithms. But commonly used are the correct classification rate and confusion matrix. The number of correct predictions divided by the total number of samples will give the correct classification rate of the algorithm. This criterion will provide a correct interpretation when the samples belonging to each class are equal. It is calculated with the following formula.

$$\text{Doğru sınıflandırma oranı} = \frac{\text{Doğru sınıflandırılan örnek sayısı}}{\text{Toplam örnek sayısı}}$$

The confusion matrix is used to examine the classification success in more detail. This criterion indicates the full performance of the model. It can also be called an error matrix. The confusion matrix for a binary classification would be as follows.

TABLE I
CONFUSION MATRIX

	Prediction Values	
Actual Values	TN	FP
	FN	TP

The abbreviations in this matrix will be as follows.

- True Positives (TP): These are examples where the true value is 1 and the predicted value is 1. So it was predicted correctly.
- True Negatives (TN): These are instances where the true value is 0 and the predicted value is 0. So it was predicted correctly.
- False Positives (FP): These are instances where the predicted value is 1 while the true value is 0. So it was guessed wrong.

- False Negatives (FN): These are instances where the predicted value is 0 while the true value is 1. So it was guessed wrong.

Many different success measures can be calculated from the values on this matrix. The aim here is to increase the values in the correctly guessed cross column and decrease the values outside it.

III. RESULTS

A. Statistical Findings

File names were used to make various statistical calculations according to the collected person information of the data. Each data in the image filenames was parsed and subjected to simple statistical analysis. When the image data obtained in the study is examined according to gender values, it is seen that the majority of them are women. The whole sample consists of 1597 male (40%) and 2358 female (60%) data. This is illustrated visually in the figure below.

TABLE II
DISTRIBUTION OF DATA BY GENDER AND AGE

Gender	Person Number	Age
		Min-Max (Avg±Std.)
Male	40	10- 68 (31.12 ± 15.85)
Female	59	10- 71 (22.96 ± 12.08)
Total	99	10-71 (26.26 ± 14.23)

When the distribution of the data by age is examined, it is seen that there are different numbers of people in this range, the youngest being 10 years old and the oldest 71 years old, and it is predominantly under 25 years old. In the figure below, the distribution of the number of people of each age is given graphically. Here, it is seen that the data is especially high in the 10-20 age range and the density is very low in the 40-72 age range. It should be noted that the data here is not the number of people, but the number of images obtained from each person.

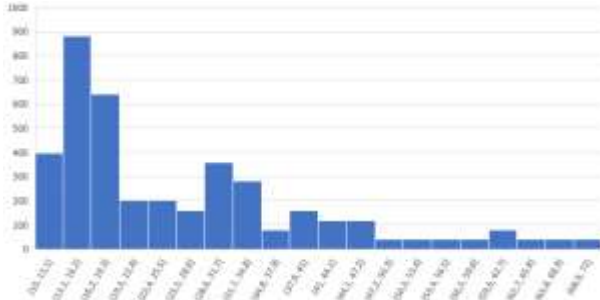


Fig. 6. Graph showing how many people are of each age

B. Person Classification Findings

There are different numbers of image data belonging to a total of 100 people. All these data are feature extracted with MRELBP. Classification algorithms were used to determine who among the 100 people on these images were. The classification rates obtained by using 32 different classification algorithms in the Matlab program and the names are given in the table below. Subspace has the highest classification success compared to other classification algorithms. It was obtained as 91.4% with the discriminant algorithm. Among other algorithms other than this, there are algorithms that find success

below or above 80%. Here, some algorithms could not produce results and therefore a total of 28 algorithms were used. Classification processes produce different results each time they run, but for this study, each algorithm was run only once.

TABLE III
PERSON CLASSIFICATION RESULTS

Algorithm Group	Algorithm Name	Accuracy rate (%)
Decision Trees	Fine Tree	38.4
	Medium Tree	15.5
	Coarse Tree	4.9
Naive Bayesian	Kernel Naive Bayesian	58.9
SVM	Linear SVM	83.5
	Quadratic SVM	86.9
	Cubic SVM	85.7
	Fine Gaussian SVM	16.9
	Medium Gaussian SVM	76.3
	Coarse Gaussian SVM	64.5
Nearest Neighbor	Fine KNN	82.8
	Medium KNN	77.5
	Coarse KNN	51.4
	Cosine KNN	74.8
	Cubic KNN	64.4
	Weighted KNN	81.6
Ensemble	Boosted Trees	30.2
	Bagged Trees	85.8
	Subspace Discriminant	91.4
	Subspace KNN	79.3
	Rusboosted Trees	22.3
Neural Network	Narrows Neural Network	70.8
	Medium Neural Network	85.2
	Wide Neural Network	89
	Bilayered Neural Network	63
	Tripping Neural Network	55.7
Kernel Aproximation	Svm Kernel	74.9
	Logistics Regression Kernel	63

Since there are 100 people in total, the error matrix is very large. The error matrix is given below, but the values in the table cannot be read. Faulty points are shown with different colors. Out of a total of 3955 samples, only 339 were misclassified. This shows that a very high classification success has been achieved.

C. Gender Classification Findings

29 different algorithms were used to classify the images of the inner surface and outer surface of the hand as male or female.

Bagged, one of the highest accuracy ensemble algorithms It was obtained as 92.6% with the Trees algorithm. When the classification successes of other algorithms are examined, it is seen that many algorithms have an accuracy rate of over 90%. The results obtained in the table below are given as a percentage with the names of the algorithms. The row with the highest success rate is marked in color.

TABLE IV
GENDER CLASSIFICATION RESULTS

Algorithm Group	Algorithm Name	Accuracy rate (%)
Decision Trees	Fine Tree	79.7
	Medium Tree	73.7
	Coarse Tree	66.8
Logistics Regression	Logistics Regression	79.2
Naive Bayesian	Kernel Naive Bayesian	69.1
SVM	Linear SVM	79.8
	Quadratic SVM	90.8
	Cubic SVM	93.7
	Fine Gaussian SVM	76.5
	Medium Gaussian SVM	89.4
	Coarse Gaussian SVM	70.7
Nearest Neighbor	Fine KNN	94.7
	Medium KNN	90.9
	Coarse KNN	77.2
	Cosine KNN	91.1
	Cubic KNN	86
	Weighted KNN	92.7
Ensemble	Boosted Trees	87.5
	Baggaed Trees	92.6
	Subspace Discriminant	83.7
	Subspace KNN	92.4
	Rusboosted Trees	84.4
Neural Network	Narrows Neural Network	90
	Medium Neural Network	91.2
	Wide Neural Network	91.8
	Bilayered Neural Network	90.3
	Tripping Neural Network	88.9
Kernel Aproximation	Svm Kernel	88.1
	Logistics Regression Kernel	84

Baggaed in gender classification The error matrix of the results obtained by the Trees algorithm is given in the table below. Here, it is seen that the distribution of the data is not uniform and there are more samples in female data. However, the classification algorithm performed well and achieved a high accuracy rate. In total, only 291 samples were misclassified. Of these, 121 were misclassified as male when they were female, and 170 were misclassified as female while male.

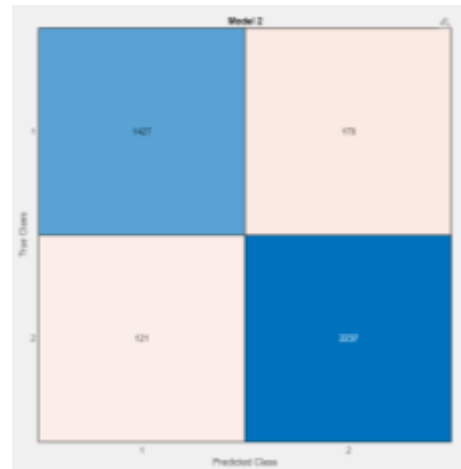


Fig. 7. error matrix of Baggaed trees algorithm for sex classification

D. Age Classification Findings

The ages of the people vary between 10 and 71 in different numbers. The distribution of these values has been given in the previous chapters. Although this distribution is not close to each other, the algorithms in the Matlab program have shown a high level of learning. Wide under the category of The Neural Network algorithm achieved a successful classification rate of 85.9%. There have also been different algorithms that produce learning results close to this value. But at the same time, algorithms that produce results with a very low success rate attract attention. The obtained results are given in the table below in a grouped way. The row with the highest success rate is marked in color.

TABLE V
AGE CLASSIFICATION RESULTS

Algorithm Group	Algorithm Name	Accuracy rate (%)
Decision Trees	Fine Tree	46.4
	Medium Tree	28.4
	Coarse Tree	16.1
Naive Bayesian	Kernel Naive Bayesian	43.5
SVM	Linear SVM	73.4
	Quadratic SVM	84
	Cubic SVM	84.7
	Fine Gaussian SVM	20.3
	Medium Gaussian SVM	72.7
	Coarse Gaussian Svm	39.8
Nearest Neighbor	Fine KNN	84.4
	Medium KNN	79.7
	Coarse KNN	52.1
	Cosine KNN	77.5
	Cubic KNN	66.9
	Weighted KNN	82.9
Ensemble	Boosted Trees	37.8
	Baggaed Trees	84.9

	Subspace Discriminant	79.3
	Subspace KNN	80.7
	Rusboosted Trees	20.8
Neural Network	Narrows Neural Network	62.6
	Medium Neural Network	79.7
	Wide Neural Network	85.9
	Bilayered Neural Network	57.9
	Tripping Neural Network	52.7
Kernel Aproximation	Svm Kernel	73.5
	Logistics Regression Kernel	51.2

It was stated in the previous titles that the age values are more between 10 and 25. For this reason, when the error matrix given in the figure below is examined, it will be seen that the erroneous estimations are concentrated here. However, despite all this, only 518 out of 3955 samples were misclassified. The remaining sample was all correctly classified.

IV. DISCUSSION AND CONCLUSION

In this study, it was aimed to determine who the people are, how old they are and what gender they are from the inner and outer surface images of their hands. For this purpose, 3955 images were collected from 100 different people. The features of these images were extracted with the median robust extended local binary model (MRELBP) method and classification was performed with many different algorithms in the Matlab program. While an accuracy rate of 91.4% was obtained for person recognition, a success rate of 92.6% was obtained for gender. Finally, a classification success rate of 85.9% was achieved for age. All these results show that it is possible to make recognition from the inner and outer surface images of the hand with high success with the method here. In the examinations made in the literature, no source directly similar to the study here was found. However, 99.7% person recognition was made with the VGG19 transfer learning algorithm on the vein images on the outer surface of the hand [33]. Although this study considers the outer surface of the hand, it is completely different from the study here. It is thought that with the effect of the transfer learning algorithm used, it may have obtained higher results than the study here. In a study conducted by Afifi [34], gender recognition study was carried out from hand images using deep learning methods. Both the inner surface and the outer surface of the hand were analyzed separately. It achieved a classification success of 94.2% in gender recognition for the inner surface of the hand and 97.3% in gender recognition for the outer surface of the hand. It is thought that this study produced higher results than the study here, because it evaluates the inner and outer surfaces of the hand separately. Al-johania and Elrefaei [35], applied deep learning algorithms on data with 500 images in one of two different datasets and 1575 images in the other, and obtained a 100% recognition rate for person recognition and a 99.25% recognition rate in another dataset. In this study, it is thought that the higher data and the feature extraction method used

cause this high recognition rate. There are many studies for person recognition from hand vein images [36-40]. However, since these studies are not directly related to the present study, they have not been compared in detail.

ACKNOWLEDGMENTS

This study was presented as a master's thesis at Kırşehir Ahi Evran University, Institute of Science and Technology.

REFERENCES

- [1] M. M. J. A. S. E. J. Fahmy, "Palmprint recognition based on Mel frequency Cepstral coefficients feature extraction," vol. 1, no. 1, pp. 39-47, 2010.
- [2] M. A. Alsmirat, F. Al-Alem, M. Al-Ayyoub, Y. Jararweh, and B. Gupta, "Impact of digital fingerprint image quality on the fingerprint recognition accuracy," *Multimedia Tools and Applications*, vol. 78, no. 3, pp. 3649-3688, 2019.
- [3] H. Chen and B. Bhanu, "Contour matching for 3D ear recognition," in *2005 Seventh IEEE Workshops on Applications of Computer Vision (WACV/MOTION'05)-Volume 1*, 2005, vol. 1: IEEE, pp. 123-128.
- [4] Ž. Emeršič, V. Štruc, and P. Peer, "Ear recognition: More than a survey," *Neurocomputing*, vol. 255, pp. 26-39, 2017.
- [5] M. Fischer, M. Rybnicek, and S. Tjoa, "A novel palm vein recognition approach based on enhanced local Gabor binary patterns histogram sequence," in *2012 19th International Conference on Systems, Signals and Image Processing (IWSSIP)*, 2012: IEEE, pp. 429-432.
- [6] C. Wilson, *Vein pattern recognition: a privacy-enhancing biometric*. CRC press, 2010.
- [7] W. Shu and D. Zhang, "Automated personal identification by palmprint," *Optical Engineering*, vol. 37, pp. 2359-2362, 1998.
- [8] A. Michele, V. Colin, and D. D. J. P. C. S. Santika, "Mobilenet convolutional neural networks and support vector machines for palmprint recognition," vol. 157, pp. 110-117, 2019.
- [9] X.-Q. Wu, K.-Q. Wang, and D. Zhang, "Wavelet based palm print recognition," in *Proceedings. International Conference on Machine Learning and Cybernetics*, 2002, vol. 3: IEEE, pp. 1253-1257.
- [10] S. F. ABD RAZAK, "IMAGE ANALYSIS OF PALM (PALMISTRY)(HEALTH AND CHARACTERISTICS)," BACHELOR OF ENGINEERING, ELECTRICAL & ELECTRONICS ENGINEERING, Universiti Teknologi PETRONAS, TRONOH, PERAK, 2006.
- [11] J. Saint-Germain, *Lovers Guide to Palmistry: Finding Love in the Palm of Your Hand*. Llewellyn Worldwide, 2008.
- [12] M. M. Houck and J. A. Siegel, *Fundamentals of forensic science*. Academic Press, 2009.
- [13] A. R. Jackson and J. M. Jackson, *Forensic science*. Pearson Education, 2008.
- [14] A. Younesi and M. C. J. P. C. S. Amirani, "Gabor filter and texture based features for palmprint recognition," vol. 108, pp. 2488-2495, 2017.
- [15] A. K. Jain, A. Ross, and S. Prabhakar, "An introduction to biometric recognition," *IEEE Transactions on circuits and systems for video technology*, vol. 14, no. 1, pp. 4-20, 2004.
- [16] Y. Bulatov, S. Jambawalikar, P. Kumar, and S. Sethia, "Hand recognition using geometric classifiers," in *International Conference on Biometric Authentication*, 2004: Springer, pp. 753-759.
- [17] L. Fei, B. Zhang, W. Zhang, and S. J. I. S. Teng, "Local apparent and latent direction extraction for palmprint recognition," vol. 473, pp. 59-72, 2019.
- [18] J. Cui, "Multispectral fusion for palmprint recognition," *Optik-International Journal for Light*, vol. 124, no. 17, pp. 3067-3071, 2013.
- [19] S. Zhang and X. Gu, "Palmprint recognition method based on score level fusion," *Optik-International Journal for Light and Electron Optics*, vol. 124, no. 18, pp. 3340-3344, 2013.
- [20] S. Zhang and X. Gu, "Palmprint recognition based on the representation in the feature space," vol. 124, no. 22, pp. 5434-5439, 2013.
- [21] J. Li, J. Cao, and K. Lu, "Improve the two-phase test samples representation method for palmprint recognition," *Optik*, vol. 124, no. 24, pp. 6651-6656, 2013.
- [22] S. Zhao and B. Zhang, "Deep discriminative representation for generic palmprint recognition," *Pattern Recognition*, vol. 98, p. 107071, 2020.

- [23] W. M. Matkowski, T. Chai, and A. W. K. Kong, "Palmprint recognition in uncontrolled and uncooperative environment," *IEEE Transactions on Information Forensics Security*, vol. 15, pp. 1601-1615, 2019.
- [24] Z. Liu, Y. Yin, H. Wang, S. Song, and Q. Li, "Finger vein recognition with manifold learning," *Journal of Network Computer Applications*, vol. 33, no. 3, pp. 275-282, 2010.
- [25] D. Hong, W. Liu, J. Su, Z. Pan, and G. Wang, "A novel hierarchical approach for multispectral palmprint recognition," *Neurocomputing*, vol. 151, pp. 511-521, 2015.
- [26] M. D. Bounneche, L. Boubchir, A. Bouridane, B. Nekhou, and A. Ali-Chérif, "Multi-spectral palmprint recognition based on oriented multiscale log-Gabor filters," *Neurocomputing*, vol. 205, pp. 274-286, 2016.
- [27] F. Ma, X. Zhu, C. Wang, H. Liu, and X.-Y. Jing, "Multi-orientation and multi-scale features discriminant learning for palmprint recognition," *Neurocomputing*, vol. 348, pp. 169-178, 2019.
- [28] D. Tamrakar, P. J. J. o. V. C. Khanna, and I. Representation, "Kernel discriminant analysis of Block-wise Gaussian Derivative Phase Pattern Histogram for palmprint recognition," vol. 40, pp. 432-448, 2016.
- [29] D. Hong, W. Liu, X. Wu, Z. Pan, and J. Su, "Robust palmprint recognition based on the fast variation Vese-Osher model," *Neurocomputing*, vol. 174, pp. 999-1012, 2016.
- [30] C. Turan and K.-M. Lam, "Histogram-based local descriptors for facial expression recognition (FER): A comprehensive study," *Journal of visual communication and image representation*, vol. 55, pp. 331-341, 2018.
- [31] T. TUNCER and A. J. T. B. V. B. v. M. D. Engin, "Yerel İkili Örüntü Tabanlı Veri Gizleme Algoritması: LBP-LSB," vol. 10, no. 1, pp. 48-53, 2017.
- [32] L. Liu, S. Lao, P. W. Fieguth, Y. Guo, X. Wang, and M. J. I. T. o. I. P. Pietikäinen, "Median robust extended local binary pattern for texture classification," vol. 25, no. 3, pp. 1368-1381, 2016.
- [33] H. Wan, L. Chen, H. Song, and J. Yang, "Dorsal hand vein recognition based on convolutional neural networks," in *2017 IEEE International Conference on Bioinformatics and Biomedicine (BIBM)*, 2017: IEEE, pp. 1215-1221.
- [34] M. Afifi, "11K Hands: Gender recognition and biometric identification using a large dataset of hand images," *Multimedia Tools and Applications*, vol. 78, no. 15, pp. 20835-20854, 2019.
- [35] N. A. Al-johania and L. A. Elrefaei, "Dorsal hand vein recognition by convolutional neural networks: Feature learning and transfer learning approaches," *International Journal of Intelligent Engineering and Systems*, vol. 12, no. 3, pp. 178-91, 2019.
- [36] S.-J. Chuang, "Vein recognition based on minutiae features in the dorsal venous network of the hand," *Signal, Image and Video Processing*, vol. 12, no. 3, pp. 573-581, 2018.
- [37] S. A. Radzi, M. K. Hani, and R. Bakhteri, "Finger-vein biometric identification using convolutional neural network," *Turkish Journal of Electrical Engineering & Computer Sciences*, vol. 24, no. 3, pp. 1863-1878, 2016.
- [38] L. Wang, G. Leedham, and S.-Y. Cho, "Infrared imaging of hand vein patterns for biometric purposes," *IET computer vision*, vol. 1, no. 3-4, pp. 113-122, 2007.
- [39] L. Wang, G. Leedham, and D. S.-Y. Cho, "Minutiae feature analysis for infrared hand vein pattern biometrics," *Pattern recognition*, vol. 41, no. 3, pp. 920-929, 2008.
- [40] O. O. Iroanya, T. F. Egwuatu, O. T. Talabi, and İ. S. Ogunleye. "Sex Prediction Using Finger, Hand and Foot Measurements for Forensic Identification in a Nigerian Population". *Sakarya University Journal of Science*, vol. 24 no. 3, pp. 432-445, 2020.

BIOGRAPHIES



EMRAH AYDEMİR Elazig, in 1987. He received the M.S. degrees in computer teaching from the University of Elazig Firat, in 2012 and the Ph.D. degree in informatics from Istanbul University, Turkey, TR, in 2017. From 2012 to 2015, he was an Expert with the Istanbul Commerce University. Since 2017, he has been an Associate Professor with the management information systems, Sakarya University. He is the author of three books, more than 10 articles, and more than 40 conference presentation. His research interests include artificial intelligence, microcontroller, database and software.

RAGHAD TOHMAS ESFANDIYAR ALALAWI She received the B.S. in computer engineering from the University in Iraq. She completed her master's degree in Advanced Technologies at Kırşehir Ahi Evran University. She works on artificial intelligence and image processing.